

A Metal and Nitrogen doped Carbon Composite with Both Oxygen Reduction and Evolution Active Sites for Rechargeable Zinc-air Batteries

Jinjie Fang, Xuejiang Zhang, Xingdong Wang, Di Liu, Yanrong Xue, Zhiyuan Xu,
Yufeng Zhang, Chun Song, Wei Zhu and Zhongbin Zhuang*

Supplementary Information

Experimental details

Chemicals

All chemicals were used as received without further purification. Zinc nitrate hexahydrate ($\text{Zn}(\text{NO}_3)_2 \cdot 6\text{H}_2\text{O}$), potassium hydroxide (KOH, 99.99%), N,N-Dimethylformamide (DMF, 99.5%), thionyl chloride (SOCl_2 , 99.5%) and poly(ethyleneimine) (PEI, 99%) were purchased from Aladdin. Ferric chloride (FeCl_3), nickel nitrate hexahydrate ($\text{Ni}(\text{NO}_3)_2 \cdot 6\text{H}_2\text{O}$), potassium permanganate (KMnO_4), sulfuric acid (H_2SO_4 , 98%), hydrogen peroxide (H_2O_2 , 30%), hydrochloric acid (HCl, >36%), methanol (MeOH, AR) and ethanol (EtOH, AR) were obtained from Sinopharm Chemical Ltd. 2-methylimidazole (2-MIM, 98%) and tetrahydrofuran (THF, 99.0%) were purchased from Macklin. Graphitized multi-walled carbon nanotube (GMWCNT, 99.5%) were supplied by XFNANO. Commercial Pt/C (20 wt.% Pt), Nafion solution (5 wt.%) and IrO_2 (99.9%) were purchased from Alfa Aesar. Carbon fiber paper (SGL 29BC) was supplied by SGL. All the water used in the experiments was ultrapure water ($\geq 18.2 \text{ M}\Omega \text{ cm}^{-1}$).

Material Preparation

Preparation of PEI/CNT: Firstly, the moderate oxidized carbon nanotube (O-CNT) was prepared by a modified Hummers method published by Dai et al, where the consumption of KMnO_4 is 2 g. Secondly, 200 mg of O-CNT was dissolved in 82 of ml DMF under sonication for 15 min to build up a homogenous solution. Then, this solution was placed in an ice bath ($\sim 5^\circ \text{C}$), following by adding 18 ml of SOCl_2 dropwise into it with vigorous stirring for 30 min. After that, the solution was transfer to an oil bath at 80°C for 12 hours with vigorous stirring. The resultant products were separated by centrifuge as well as washed by THF three times and DMF twice. Then, the above products were dispersed in 80 ml DMF in 250 ml round-bottom flask under sonication for 1 hour to form a homogenous solution (Solution A). 3 g of PEI was dispersed in 20 ml DMF under sonication for 1 hour to form a homogenous solution (Solution B).

Solution B was added into Solution A, followed by transferring the mixing solution to an oil bath at 60°C for 12 hours with vigorous stirring. The resultant products were separated by filtration, washed by EtOH twice. After dispersing the precipitate in 100 ml of water and lyophilizing it, the PEI/CNT was synthesized.

Preparation of Fe,Ni-N-C/O-CNT: The preparation of Fe,Ni-N-C/O-CNT followed the same procedure as Fe,Ni-N-C/N-CNT without dispersing PEI/CNT in Solution A but 30 mg of O-CNT.

Preparation of Fe,Ni-N-C: The preparation of Fe,Ni-N-C followed the same procedure as Fe,Ni-N-C/N-CNT without dispersing PEI/CNT in Solution A.

Preparation of Fe-N/C-NCNT: The preparation of N/C-NCNT followed the same procedure as Fe,Ni-N-C/N-CNT without dissolving FeCl₃ in Solution A.

Preparation of Ni-N/C-NCNT: The preparation of N/C-NCNT followed the same procedure as Fe,Ni-N-C/N-CNT without dissolving Ni(NO₃)₂·6H₂O in Solution A.

Preparation of N/C-NCNT: The preparation of N/C-NCNT followed the same procedure as Fe,Ni-N-C/N-CNT without dissolving FeCl₃ and Ni(NO₃)₂·6H₂O in Solution A.

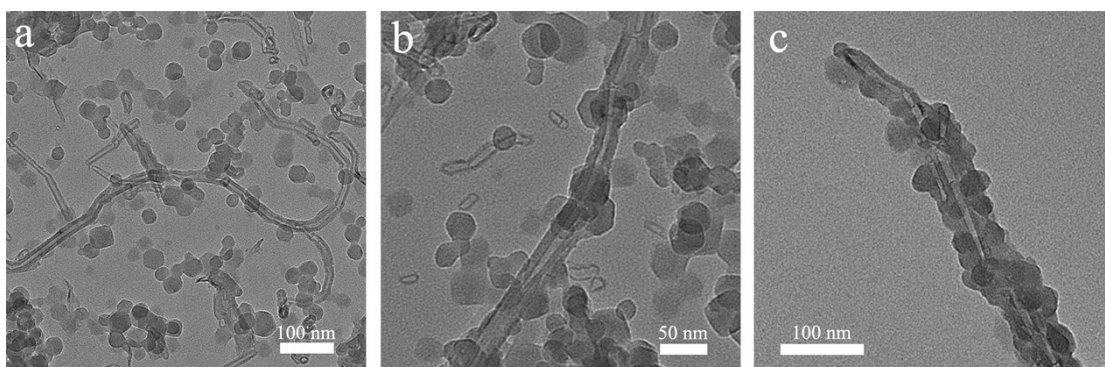


Figure S1. TEM image of the Fe,Ni-ZIF-8/PEI/CNT precursor.

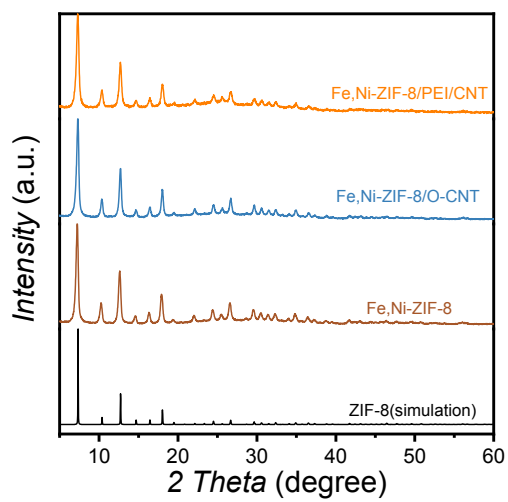


Figure S2. XRD patterns of the obtained precursors.

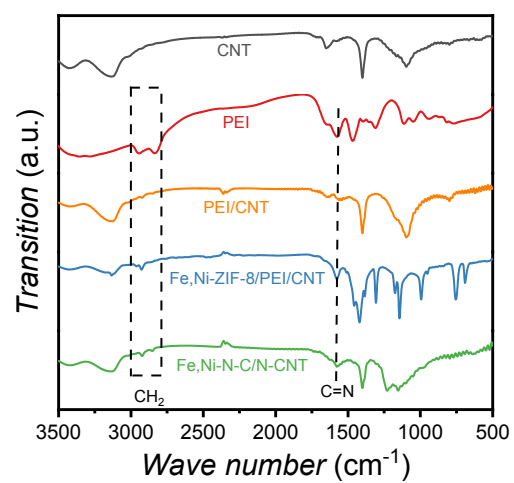
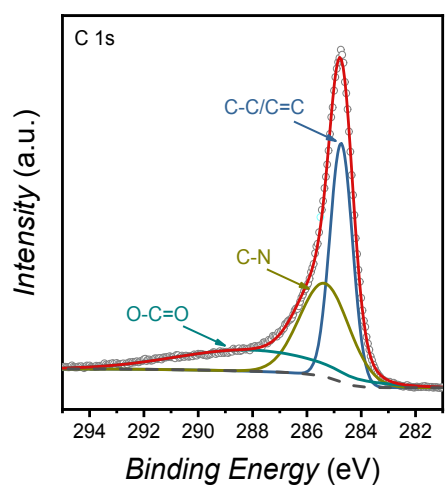


Figure S3. FT-IR spectra of O-CNT, PEI/CNT, PEI, Fe,Ni-ZIF-8/PEI/CNT and Fe,Ni-N-C/N-CNT, respectively.



a

Figure S4. High resolution C 1s XPS spectra of the Fe,Ni-N-C/N-CNT.

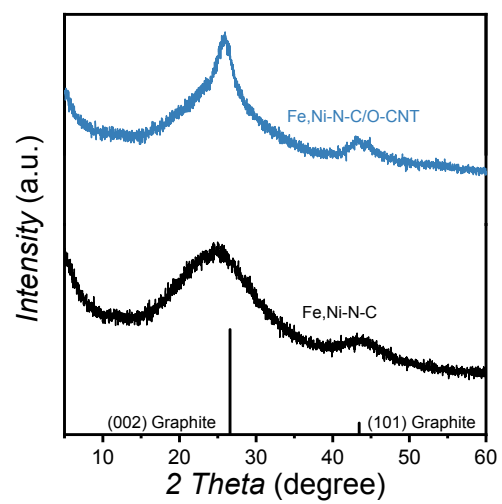


Figure S5. XRD patterns of the Fe,Ni-N-C/O-CNT and Fe,Ni-N-C.

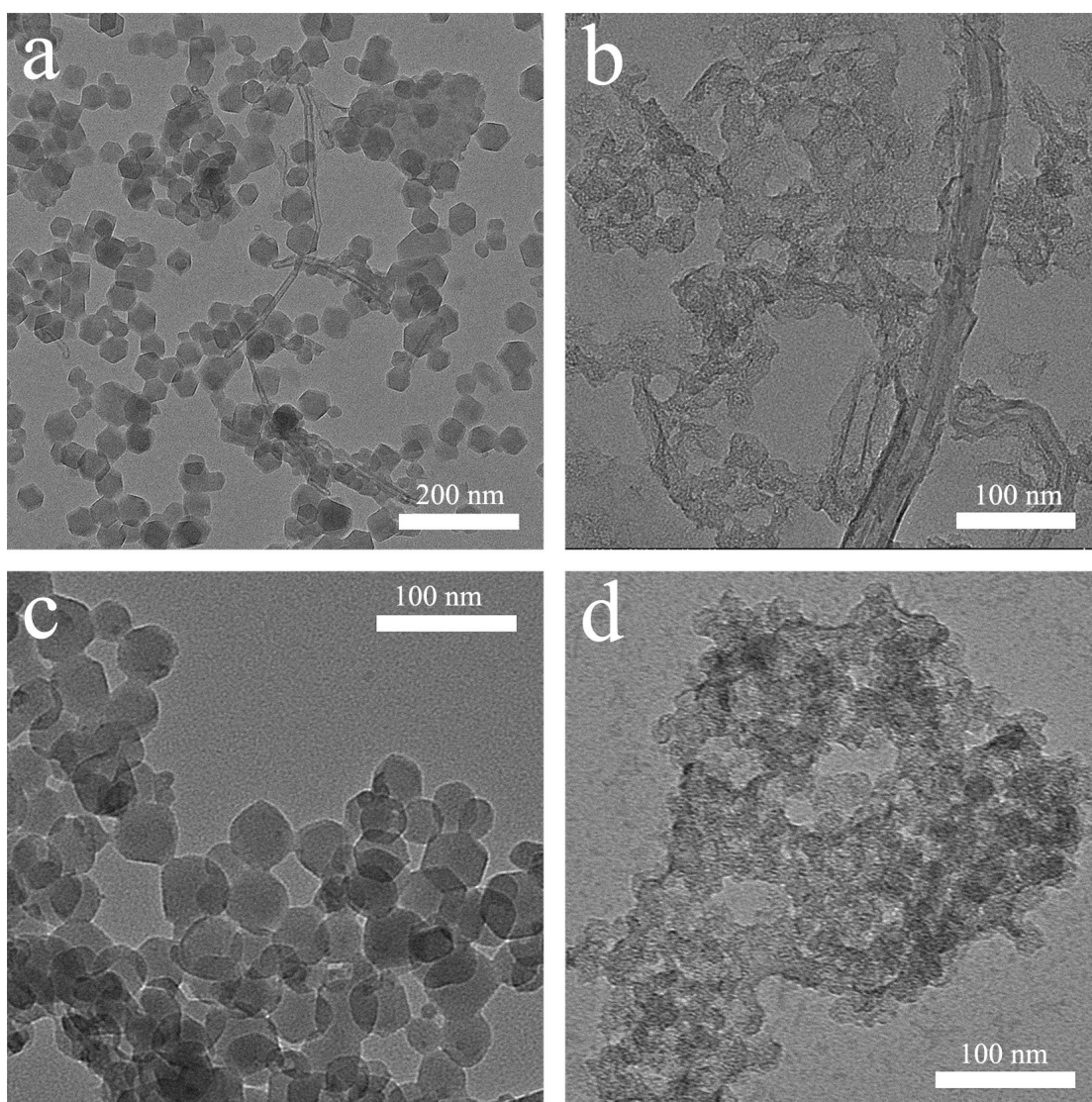


Figure S6. TEM images of a) Fe,Ni-ZIF-8/O-CNT. b) Fe,Ni-N-C/O-CNT. c) Fe,Ni-ZIF-8. d) Fe,Ni-N-C.

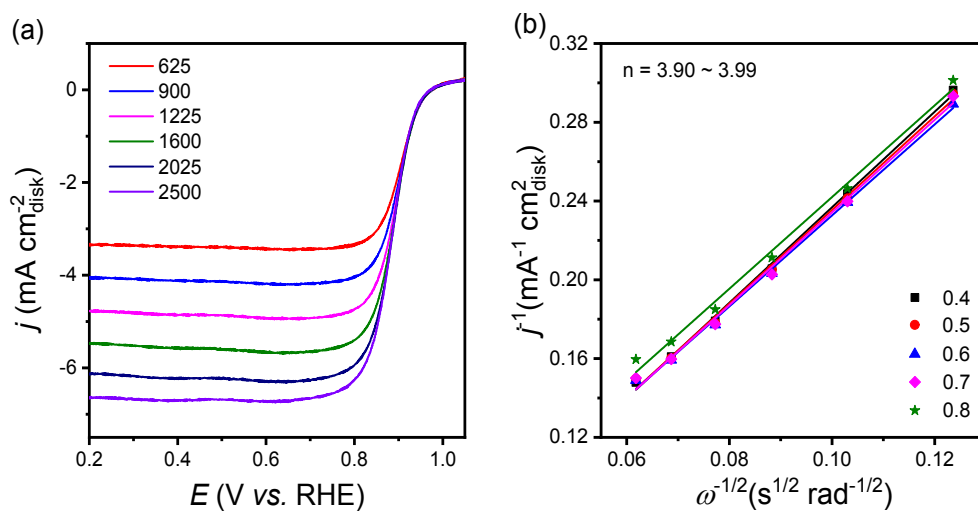


Figure S7. a) The ORR polarization curves at different rotating rates of the Fe, Ni-N-C/N-CNT, b) K-L plots and electron-transfer numbers.

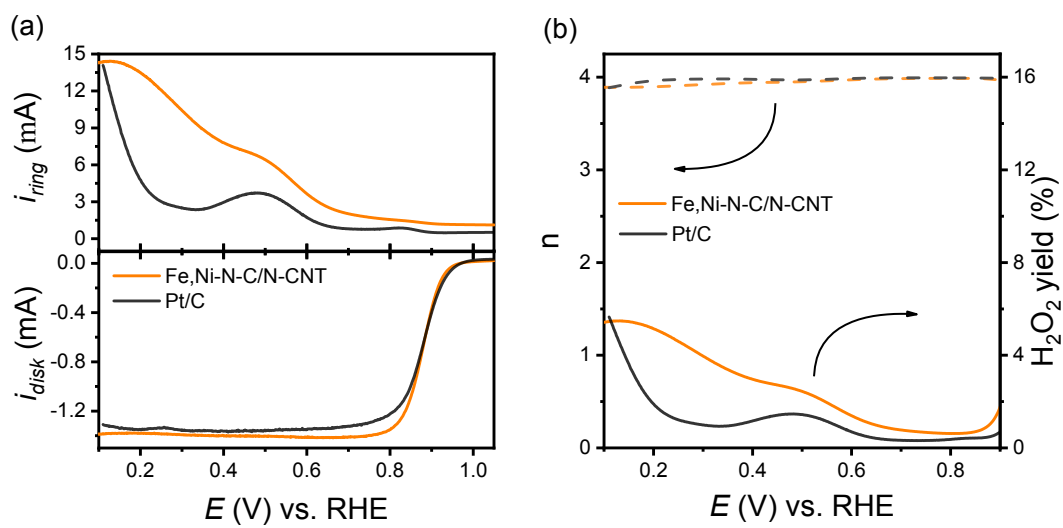


Figure S8. a) RRDE testing results of Fe,Ni-N-C/N-CNT and Pt/C. b) The electron transfer number and yield of hydrogen peroxide of Fe,Ni-N-C/N-CNT and Pt/C.

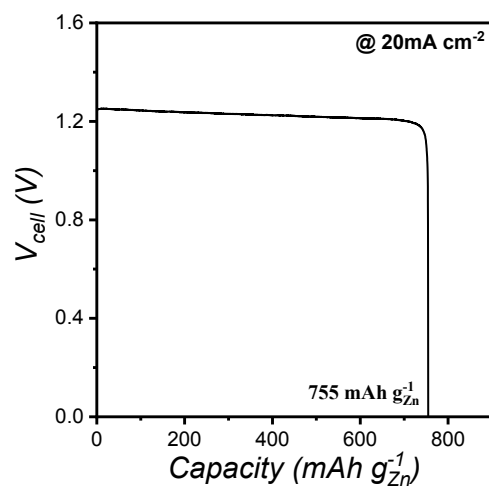


Figure S9. Specific capacity of the Fe,Ni-N-C/N-CNT ZAB at the current density of 20 mA cm^{-2} .

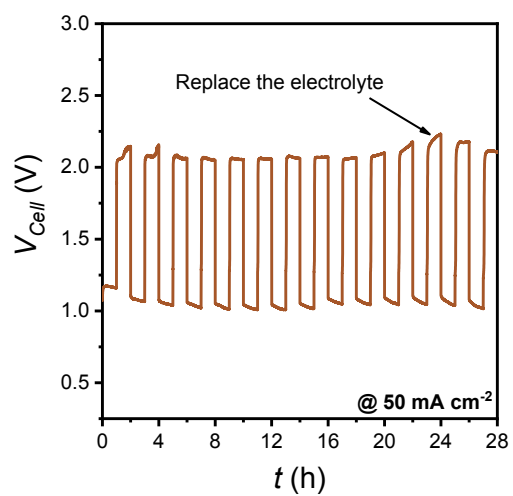


Figure S10. Galvanostatic discharge-charge cycling profiles of the FeNi-N-C/N-CNT ZAB at current density of 50 mA cm⁻² with a cycling interval of 2 h.

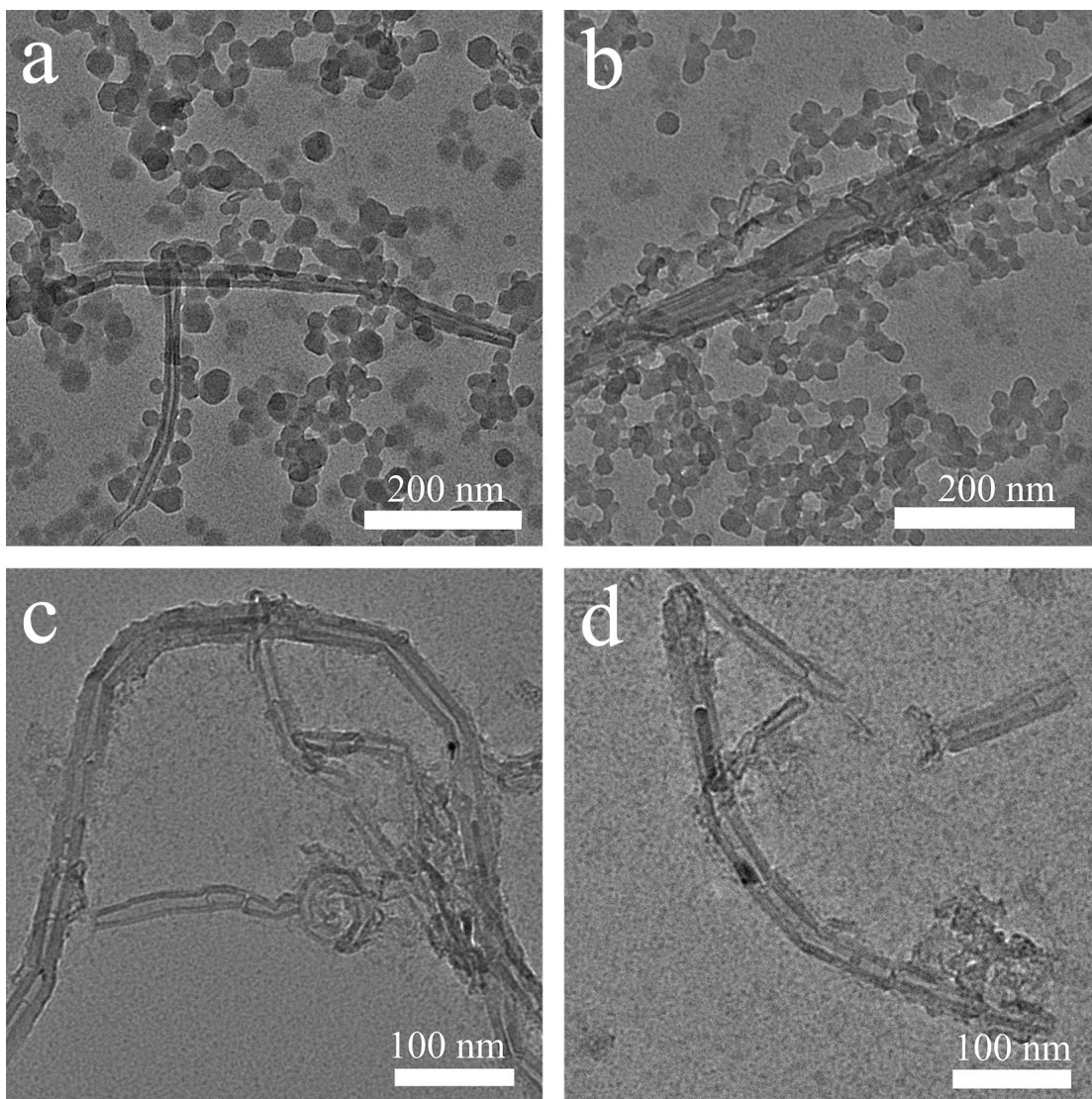


Figure S11. a) TEM images of a) Fe-ZIF-8/PEI/CNT. b) Ni-ZIF-8/PEI/CNT. c) Fe-N-C/N-CNT. d) Ni-N-C/N-CNT.

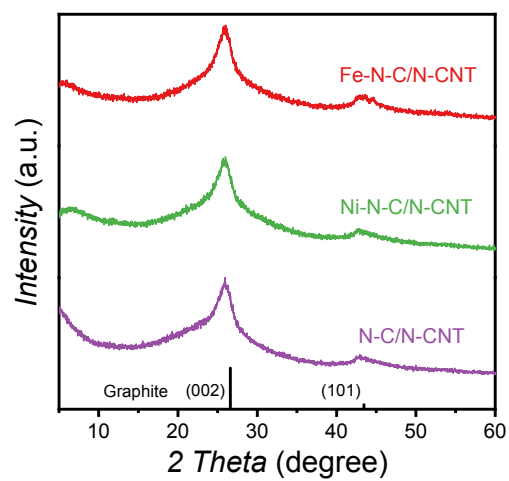


Figure S12. XRD patterns of the Fe-N-C/N-CNT, Ni-N-C/N-CNT and N-C/N-CNT.

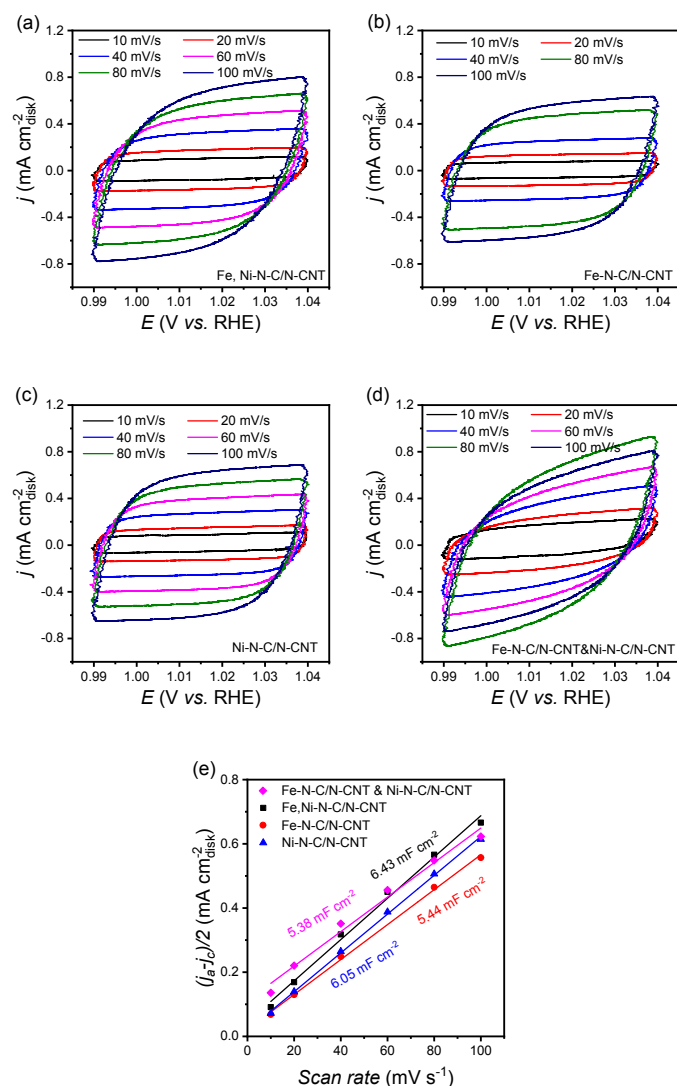


Figure S13. Cyclic voltammetry of a) Fe, Ni-N-C/N-CNT b) Fe-N-C/N-CNT c) Ni-N-C/N-CNT and d) Fe-N-C/N-CNT & Ni-N-C/N-CNT at different scan rate. e) The plots of current density versus scan rate.

The electrochemically active surface area (ECSA) was evaluated based on the double layer capacitance (C_{dl}) in the non-Faradaic potential region. Specifically, the C_{dl} was tested via CV measurements at various scan rates (10, 20, 40, 60, 80, and 100 mV s^{-1}). The C_{dl} was obtained by the slope from the plots of $(j_a - j_c)/2$ at 1.015 V (where j_a and j_c are the anodic and cathodic current densities, respectively) against the scan rates. The ECSA was calculated using the following equation:

$$ECSA = \frac{A \times C_{dl}}{C_s}$$

Where A is the surface area of the electrode. C_s is the specific capacitance of a smooth surface of materials under specific electrochemical condition. According to previous study, the value of C_s was 0.04 mF cm^{-2} in this calculation.

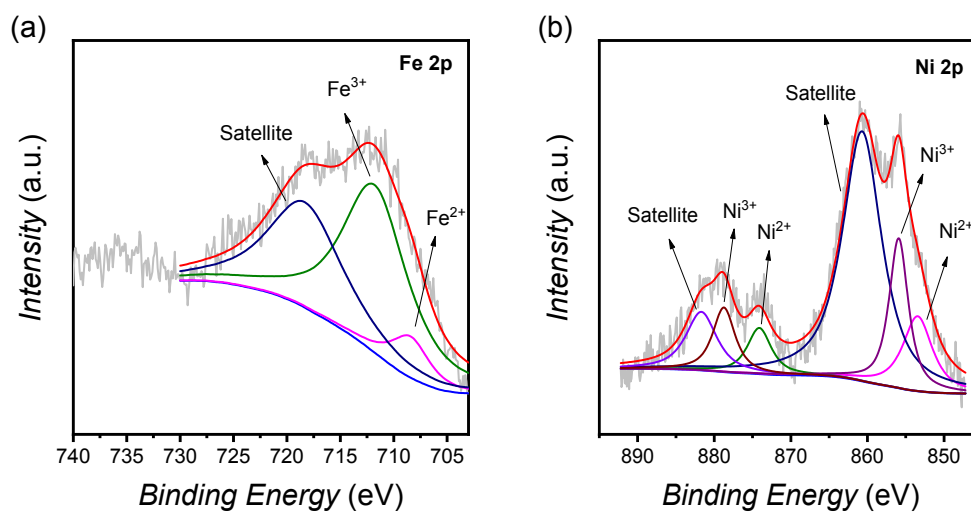


Figure S14. High resolution Fe 2p (a) and Ni 2p (b) XPS spectra of the Fe, Ni-N-C/N-CNT catalyst after OER tests.

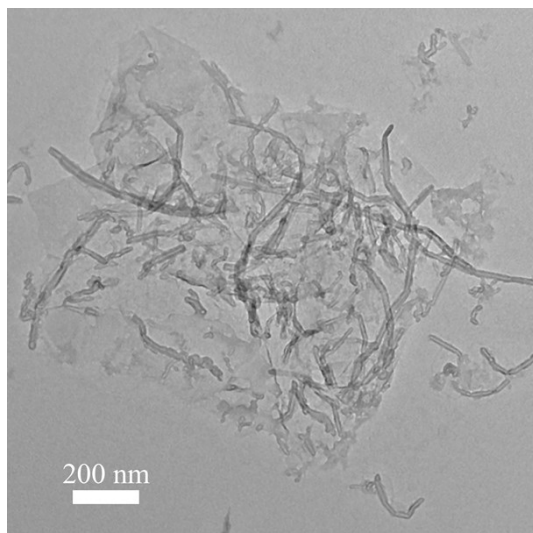


Figure S15. TEM image of acid leached Fe,Ni-N-C/N-CNT catalyst, which is after 10 h OER test.

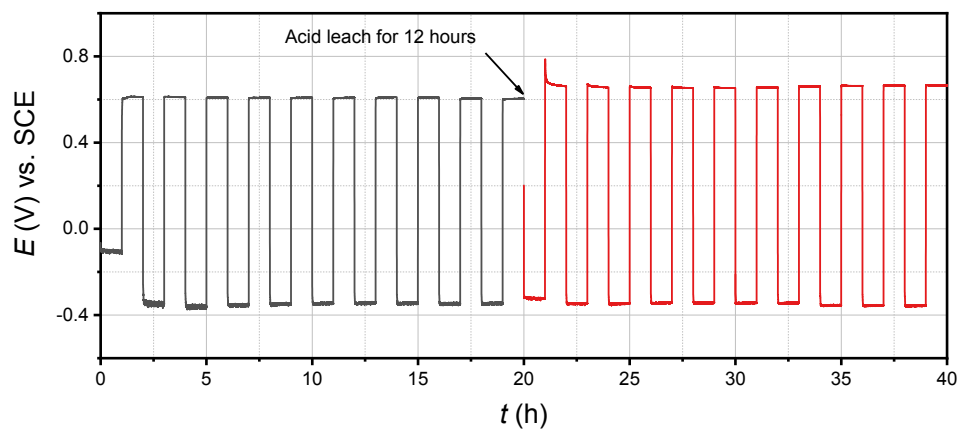


Figure S16. Galvanostatic test of Fe,Ni-N-C/N-CNT-CP at the current density of 10 mA cm^{-2} for OER and the current density of 3 mA cm^{-2} for ORR

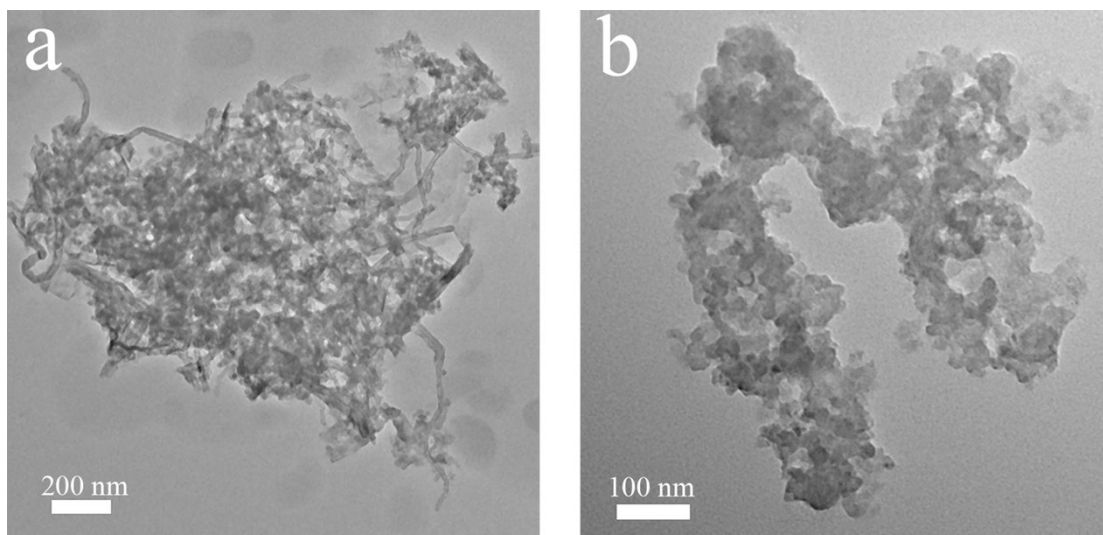


Figure S17. TEM images of a) Fe,Ni-N-C/O-CNT. b) Fe,Ni-N-C. The catalysts are after 10 h of OER tests.

Table S1. Summary of the ORR and OER activity of the bi-functional catalysts reported in the literatures.

| Electrocatalyst | Electrolyte | ORR | OER | ΔE (mV) | Reference |
|--|-------------|---------------|---|-----------------|---|
| | | $E_{1/2}$ (V) | η (mV) at $j=10$ mA cm^{-2} | | |
| FeNi-N-C/N-CNT | 0.1 M KOH | 0.879 | 315 | 666 | This work |
| | 1M KOH | 0.894 | 282 | 618 | |
| Ni-NHGF | 0.1 M KOH | 0.820 | 350 | 760 | <i>Nat. Catal.</i> 2018, 1, 63. |
| | 1 M KOH | 0.86 | 330 | 700 | |
| S ₂ N-Fe/N/C-CNT | 0.1 M KOH | 0.850 | 370 | 750 | <i>Angew. Chem. Int. Ed.</i> 2017, 56, 610. |
| Fe-N ₄ SAs/NPC | 0.1 M KOH | 0.885 | - | - | <i>Angew. Chem. Int. Ed.</i> 2018, 130, 8750. |
| | 1 M KOH | - | 430 | - | |
| Meso-CoNC@GF | 0.1 M KOH | 0.870 | 430 | 790 | <i>Adv. Mater.</i> 2018, 30, 1704898. |
| NCNFs (Co) | 0.1 M KOH | 0.870 | 370 | 730 | <i>Nat. Energy</i> 2016, 1, 15006. |
| Co-N _x /C NRA | 0.1 M KOH | 0.877 | 300 | 653 | <i>Adv. Funct. Mater.</i> 2018, 28, 1704638. |
| NiFe-LDH /Co ₂ N-CNF | 0.1 M KOH | 0.790 | 312 | 752 | <i>Adv. Energy Mater.</i> 2017, 7, 1700467. |
| CCOP _{TDP} -FeNi-SiO ₂ | 1 M KOH | 0.890 | 310 | 650 | <i>Nanoscale</i> 2019, 11, 211. |
| FeNiP/NCH | 0.1 M KOH | 0.750 | - | - | <i>J. Am. Chem. Soc.</i> 2019, 141, 7906. |
| | 1 M KOH | - | 250 | - | |
| S-GNS/NiCo ₂ S ₄ | 0.1 M KOH | 0.880 | 330 | 690 | <i>Adv. Funct. Mater.</i> 2018, 28, 1706675. |
| Co ₃ O ₄ /N-rmGO | 0.1 M KOH | 0.840 | 310 | 700 | <i>Nat. Mater.</i> 2011, 10, 780. |
| NCNT/CoFe-CoFe ₂ O ₄ | 0.1 M KOH | 0.740 | - | - | <i>ACS Appl. Mater. Interfaces</i> 2018, 10, 39828. |
| | 1 M KOH | - | 310 | - | |
| NCNT/CoO-NiO-NiCo | 1 M KOH | 0.830 | 270 | 670 | <i>Angew. Chem. Int. Ed.</i> 2015, 54, 9654. |
| MnO ₂ /CNTs | 0.1 M KOH | 0.812 | 420 | 838 | <i>ACS Appl. Mater. Interfaces</i> 2019, 11, 578. |
| CaMnO-300 | 0.1 M KOH | 0.760 | 470 | 940 | <i>Adv. Energy Mater.</i> 2018, 8, 1800612. |
| O-NGM-800 | 0.1 M KOH | 0.860 | 470 | 840 | <i>Adv. Mater.</i> 2019, 31,1803339. |

Table S2. Summary of the ZABs performance and stability reported in the literatures.

| Electrocatalysts | Peak power density (mW cm ⁻²) | ΔE at the end of test (V)* | Energy efficient (%) | Operating time and condition | Reference |
|--|---|------------------------------------|----------------------|------------------------------|--|
| FeNi-N-C/N-CNT | 273 | 0.75, 10 mA cm ⁻² | 61 | 210 h, 2 h/cycle | This work |
| FeNi-N-C/N-CNT | 273 | 1.09, 50 mA cm ⁻² | 48 | 28 h, 2 h/cycle | This work |
| Porous Fe/N/C | - | 0.90, 2 mA cm ⁻² | 51 | 10 h, 5 min/cycle | <i>ACS Sustainable Chem. Eng.</i> 2019, 7, 4030. |
| Co ₄ N/CNW/C | 173 | 0.86, 10 mA cm ⁻² | 57 | 136 h, 20 min/cycle | <i>J. Am. Chem. Soc.</i> 2016, 138, 10226. |
| Co-N ₂ B-CSs | 100 | 1.31, 5 mA cm ⁻² | 38 | 14 h, 400 s/cycle | <i>ACS Nano</i> 2018, 12, 1894. |
| FeCo-Nx-Carbon | 150 | 0.79, 10 mA cm ⁻² | 60 | 44 h, 2 h/cycle | <i>Angew. Chem. Int. Ed.</i> 2018, 57, 1856. |
| M-HIB-MOFs | 195 | 0.80, 10 mA cm ⁻² | 60 | 1000 h, 10 min/cycle | <i>Energy Environ. Sci.</i> 2019, 12, 727. |
| NiFe@N-Graphite | 85 | 0.92, 20 mA cm ⁻² | 54 | 40 h, 20 min/cycle | <i>Adv. Funct. Mater.</i> 2018, 28, 1706928. |
| NCNT/CoO-NiO-NiCo | - | 0.83, 20 mA cm ⁻² | 57 | 17 h, 20 min/cycle | <i>Angew. Chem. Int. Ed.</i> 2015, 54, 9654. |
| Co(OH) ₂ | 36 | 1.49, 15 mA cm ⁻² | 38 | 50 h, 40 min/cycle | <i>ACS Appl. Mater. Interfaces</i> 2015, 7, 12930. |
| Co/Co ₃ O ₄ @PGS | 118 | 0.96, 10 mA cm ⁻² | 51 | 800 h, 10 min/cycle | <i>Adv. Energy Mater.</i> 2018, 8, 1702900. |
| Co ₂ FeO ₄ /NCN Ts | 91 | 1.70, 50 mA cm ⁻² | 27 | 100 h, 10 min/cycle | <i>Angew. Chem. Int. Ed.</i> 2019, 58, 13291. |
| α -MnO ₂ /CNT10 | 66 | 1.20, 10 mA cm ⁻² | 48 | 50 h, 1 h/cycle | <i>Carbon</i> 2017, 111, 813. |
| MnO/Co/PGC | 172 | 0.84, 10 mA cm ⁻² | 57 | 116 h, 20 min/cycle | <i>Adv. Mater.</i> 2019, 31, 1902339. |
| CFZr(0.3)/N-rGO | - | 1.11, 15 mA cm ⁻² | 51 | 11h, 1 h/cycle | <i>ACS Catal.</i> 2018, 8, 3715. |
| LaBaSrCoFeO | - | 0.99, 10 mA cm ⁻² | 52 | 17 h, 10 min/cycle | <i>Energy Environ. Sci.</i> 2016, 9, 176. |
| 1100-CNS | 151 | 0.86, 10 mA cm ⁻² | 56 | 55 h, 10 min/cycle | <i>Energy Environ. Sci.</i> 2017, 10, 742. |
| N-doped graphene | 65 | 0.97, 2 mA cm ⁻² | 54 | 155 h, 1 h/cycle | <i>Sci. Adv.</i> 2016, 2, 1501122. |
| AgCu-NiF | 86 | 0.96, 20 mA cm ⁻² | 53 | 33 h, 20 min/cycle | <i>Electrochim. Acta</i> 2015, 158, 437. |

* ΔE is the voltage gap, $\Delta E = E_{\text{charge}} - E_{\text{discharge}}$

Table S3. High resolution N 1s XPS peak fitting results.

| Catalyst | Total pyridinic (%) | Total Nx-M (%) | Total pyrrolic (%) | Total quaternary (%) | Total graphitic (%) | total N amount (%) |
|------------------------|---------------------------|----------------------|--------------------------|----------------------------|---------------------------|-----------------------|
| FeNi-N-C/N-CNT | 0.86 | 0.80 | 1.20 | 0.90 | 0.72 | 4.5 |
| FeNi-N-C/O-CNT | 1.46 | 0.88 | 1.09 | 1.22 | 0.52 | 5.2 |
| Fe ₃ Ni-N-C | 0.70 | 0.69 | 1.05 | 0.77 | 1.34 | 4.6 |

Table S4. Raman spectra fitting results.

| Catalyst | Sp ² C outside graphene (%) | D peak (%) | Distortion, caused by C ₅ ring or heteroatoms (%) | G peak (%) | I _D /I _G |
|------------------------|---|---------------|--|---------------|--------------------------------|
| FeNi-N-C/N-CNT | 18.3 | 35.9 | 32.8 | 13.0 | 1.44 |
| FeNi-N-C/O-CNT | 17.7 | 47.6 | 14.5 | 20.2 | 1.18 |
| Fe ₃ Ni-N-C | 21.7 | 42.9 | 16.2 | 19.2 | 1.14 |